

# Energy-Efficient Power Allocation in OFDM Systems with Wireless Information and Power Transfer

Derrick Wing Kwan Ng\*, Ernest S. Lo†, and Robert Schober\*

\*Institute for Digital Communications, Universität Erlangen-Nürnberg, Germany

†Centre Tecnològic de Telecomunicacions de Catalunya - Hong Kong (CTTC-HK)

**Abstract**—This paper considers an orthogonal frequency division multiplexing (OFDM) downlink point-to-point system with simultaneous wireless information and power transfer. It is assumed that the receiver is able to harvest energy from noise, interference, and the desired signals. We study the design of power allocation algorithms maximizing the energy efficiency of data transmission (bit/Joule delivered to the receiver). In particular, the algorithm design is formulated as a high-dimensional non-convex optimization problem which takes into account the circuit power consumption, the minimum required data rate, and a constraint on the minimum power delivered to the receiver. Subsequently, by exploiting the properties of nonlinear fractional programming, the considered non-convex optimization problem, whose objective function is in fractional form, is transformed into an equivalent optimization problem having an objective function in subtractive form, which enables the derivation of an efficient iterative power allocation algorithm. In each iteration, the optimal power allocation solution is derived based on dual decomposition and a one-dimensional search. Simulation results illustrate that the proposed iterative power allocation algorithm converges to the optimal solution, and unveil the trade-off between energy efficiency, system capacity, and wireless power transfer: (1) In the low transmit power regime, maximizing the system capacity may maximize the energy efficiency. (2) Wireless power transfer can enhance the energy efficiency, especially in the interference limited regime.

## I. INTRODUCTION

Orthogonal frequency division multiplexing (OFDM) is a viable air interface for providing ubiquitous communication services and high spectral efficiency, due to its ability to combat frequency selective multipath fading and flexibility in resource allocation. However, power-hungry circuitries and the limited energy supply in portable devices remain the bottlenecks in prolonging the lifetime of networks and guaranteeing quality of service. As a result, energy-efficient mobile communication has received considerable interest from both industry and academia [1]-[4]. Specifically, a considerable number of technologies/methods such as energy harvesting and power optimization have been proposed in the literature for maximizing the energy efficiency (bit-per-Joule) of wireless communication systems. Energy harvesting is particularly appealing as it is envisioned to be a perpetual energy source which provides self-sustainability to systems.

Traditionally, energy has been harvested from natural renewable energy sources such as solar, wind, and geothermal heat, thereby reducing substantially the reliance on the energy supply from conventional energy sources. On the other hand, background radio frequency (RF) electromagnetic (EM) waves from ambient transmitters are also an abundant source of energy for energy harvesting. Indeed, EM waves can not only serve as a vehicle for carrying information, but also for carrying

energy (/power) simultaneously [5]-[8]. The utilization of this dual characteristic of EM waves leads to a paradigm shift for both receivers design and resource allocation algorithm design. In [5] and [6], the signal input distribution and the power allocation were used for achieving a trade-off between information and power transfer for different system settings, respectively. However, in [5] and [6] it was assumed that the receiver is able to decode information and extract power from the same received signal which is not yet possible in practice. As a compromise solution, the concept of a power splitting receiver was introduced in [7] and [8] for facilitating simultaneous energy harvesting and information decoding. The authors of [7] and [8] investigated the rate-energy regions for multiple antenna and single antenna narrowband systems with power splitting receivers, respectively. Nevertheless, the possibly high power consumption of both electronic circuitries and RF transmission was not taken into account in [5]-[8] but may play an important role in designing energy efficient communication systems.

In this paper, we address the above issues. To this end, we formulate the power allocation algorithm design for energy efficient communication in OFDM systems with concurrent wireless information and power transfer as an optimization problem. The resulting high-dimensional non-convex optimization problem is solved by using an iterative algorithm whose components include nonlinear fractional programming, dual decomposition, and a one-dimensional search. Simulation results illustrate an interesting trade-off between energy efficiency, system capacity, and wireless power transfer.

## II. SYSTEM MODEL

In this section, we present the adopted system model.

### A. OFDM Channel Model

We consider an OFDM system which comprises one transmitter and one receiver. The receiver is able to decode information and harvest energy from noise and radio signals (desired signal and interference signal). All transceivers are equipped with a single antenna, cf. Figure 1. The total bandwidth of the system is  $\mathcal{B}$  Hertz and there are  $n_F$  subcarriers. Each subcarrier has a bandwidth  $W = \mathcal{B}/n_F$  Hertz. We assume a frequency division duplexing (FDD) system and the downlink channel gains can be accurately obtained by feedback from the receiver. The channel impulse response is assumed to be time invariant (slow fading). The downlink received symbol at the receiver on subcarrier  $i \in \{1, \dots, n_F\}$  is given by

$$Y_i = \sqrt{P_i} g H_i X_i + I_i + Z_i^s + Z_i^a, \quad (1)$$

where  $X_i$ ,  $P_i$ , and  $H_i$  are the transmitted symbol, transmitted power, and the small-scale fading coefficient for the link from the transmitter to the receiver on subcarrier  $i$ , respectively.  $l$  and  $g$  represent the path loss and shadowing between the

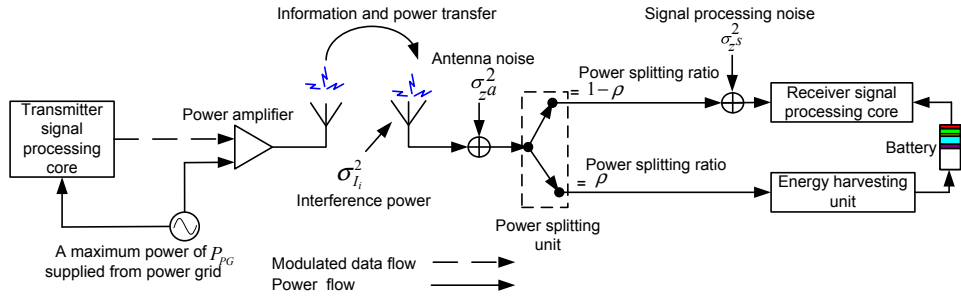


Fig. 1. OFDM transceiver model for downlink wireless information and power transfer.

transmitter and receiver, respectively.  $Z_i^s$  and  $Z_i^a$  represent the signal processing and the antenna noises on subcarrier  $i$ , respectively.  $Z_i^s$  and  $Z_i^a$  are modeled as additive white Gaussian noise (AWGN) with zero mean and variances  $\sigma_{z^s}^2$  and  $\sigma_{z^a}^2$ , respectively, cf. Figure 1.  $I_i$  is the received co-channel interference signal on subcarrier  $i$  with zero mean and variance  $\sigma_{I_i}^2$  which is emitted by an unintended transmitter in the same channel.

### B. Hybrid Information and Energy Harvesting Receiver

In practice, the energy harvesting receiver model depends on the specific implementation. For instance, both electromagnetic induction and electromagnetic radiation are able to transfer wireless power and information [6], [8]. However, the associated hardware circuitries can vary significantly. Besides, most energy harvesting circuits suffer from the half-duplex constraint in energy harvesting. Specifically, the signal used for harvesting energy cannot be used for decoding of the modulated information [8]. In order to provide a general model for a receiver which can harvest energy and decode information, we do not assume a particular type of energy harvesting receiver. Instead, we follow a similar approach as in [8] and focus on a receiver which splits the received signal into two power streams carrying a proportion of  $\rho$  and  $1 - \rho$  of the total received signal power before any active analog/digital signal processing is performed, cf. Figure 1. Subsequently, the two streams carrying a fraction of  $\rho$  and  $1 - \rho$  of the total received signal power are used for energy harvesting and decoding the information in the signal, respectively. In this paper, we assume a perfect passive power splitter unit which does not consume any power nor introduce any power loss or noise. Besides, we assume that the receiver is equipped with a battery with finite capacity for storing the harvested energy. In other words, there is a finite maximum amount of power which can be harvested by the receiver. We note that in practice, the receiver may be powered by more than one energy source and the harvested energy can be used as a supplement for supporting the energy consumption<sup>1</sup> of the receiver.

## III. RESOURCE ALLOCATION

In this section, we introduce the adopted system performance metric and formulate the corresponding power allocation problem.

### A. Instantaneous Channel Capacity

In this subsection, we define the adopted system performance measure. Given perfect channel state information (CSI) at the receiver, the channel capacity<sup>2</sup> between the transmitter and the

receiver on subcarrier  $i$  with channel bandwidth  $W$  is given by

$$C_i = W \log_2 \left( 1 + P_i \Gamma_i \right) \quad \text{and} \quad (2)$$

$$\Gamma_i = \frac{(1 - \rho) \eta g |H_i|^2}{(1 - \rho)(\sigma_{z^a}^2 + \sigma_{I_i}^2) + \sigma_{z^s}^2}, \quad (3)$$

where  $P_i \Gamma_i$  is the received signal-to-interference-plus-noise ratio (SINR) on subcarrier  $i$ . The *system capacity* is defined as the total average number of bits successfully delivered to the receiver and is given by

$$U(\mathcal{P}, \rho) = \sum_{i=1}^{n_F} C_i, \quad (4)$$

where  $\mathcal{P} = \{P_i \geq 0, \forall i\}$  is the power allocation policy and  $\rho$  is the power splitting ratio introduced in Section II-B. On the other hand, we take into account the total power consumption of the system in the objective function for designing an energy efficient power allocation algorithm. To this end, we model the power dissipation in the system as:

$$U_{TP}(\mathcal{P}, \rho) = P_C + \sum_{i=1}^{n_F} \varepsilon P_i - P_D - P_I \quad (5)$$

$$\text{where } P_D = \underbrace{\eta \sum_{i=1}^{n_F} P_i \eta g |H_i|^2 \rho}_{\text{Power harvested from desired signal}} \quad (6)$$

$$\text{and } P_I = \underbrace{\eta \sum_{i=1}^{n_F} (\sigma_{z^a}^2 + \sigma_{I_i}^2) \rho}_{\text{Power harvested from interference signal and antenna noise}}. \quad (7)$$

$P_C > 0$  is the constant *circuit signal processing power consumption* in both transmitter and receiver which includes the power dissipation in the digital-to-analog (/analog-to-digital) converter, digital/analog filters, mixer, and frequency synthesizer, and is independent of the actual transmitted or harvested power.  $\varepsilon \geq 1$  is a constant which accounts for the inefficiency of the power amplifier. For instance, 5 Watts is consumed in the power amplifier for every 1 Watt of power radiated in the radio frequency (RF) if  $\varepsilon = 5$ ; the power efficiency is  $\frac{1}{\varepsilon} = \frac{1}{5} = 20\%$ . On the other hand, the minus sign in front of  $P_D$  in (5) indicates that a portion of the power radiated by the transmitter can be harvested by the receiver.  $0 \leq \eta \leq 1$  is a constant which denotes the efficiency of the energy harvesting unit for converting the radio signal to electrical energy for storage. Specifically, the term  $\eta \eta g |H_i|^2 \rho$  in (6) can be interpreted as a *frequency selective power transfer efficiency* for transferring power from the transmitter to receiver on subcarrier  $i$ . Similarly, the minus sign in front of  $P_I$  in (5) accounts for the ability of the receiver to harvest power from interference signals and antenna noise. We note that  $U_{TP}(\mathcal{P}, \rho) > 0$  always holds

<sup>1</sup>In this paper, we use a normalized energy unit, i.e., Joule-per-second. Thus, the terms “power” and “energy” are interchangeable in this context.

<sup>2</sup>Note that the received interference signal  $I_i$  on each subcarrier is treated as AWGN which results in a lower bound of the channel capacity and is commonly done in the literature.

TABLE I  
ITERATIVE POWER ALLOCATION ALGORITHM.

**Algorithm 1** Iterative Power Allocation Algorithm

- 1: Initialize the maximum number of iterations  $L_{max}$  and the maximum tolerance  $\epsilon$
- 2: Set maximum energy efficiency  $q = 0$  and iteration index  $n = 0$
- 3: **repeat** {Main Loop}
- 4:   Solve the inner loop problem in (12) for a given  $q$  and obtain power allocation policy  $\{\mathcal{P}', \rho'\}$
- 5:   **if**  $U(\mathcal{P}', \rho') - qU_{TP}(\mathcal{P}', \rho') < \epsilon$  **then**
- 6:     Convergence = **true**
- 7:     **return**  $\{\mathcal{P}^*, \rho^*\} = \{\mathcal{P}', \rho'\}$  and  $q^* = \frac{U(\mathcal{P}', \rho')}{U_{TP}(\mathcal{P}', \rho')}$
- 8:   **else**
- 9:     Set  $q = \frac{U(\mathcal{P}', \rho')}{U_{TP}(\mathcal{P}', \rho')}$  and  $n = n + 1$
- 10:    Convergence = **false**
- 11:   **end if**
- 12: **until** Convergence = **true** or  $n = L_{max}$

*Proof:* Please refer to [4, Appendix A] for a proof similar to the one required for Theorem 1.

By Theorem 1, for any optimization problem with an objective function in fractional form, there exists an equivalent optimization problem with an objective function in subtractive form, e.g.  $U(\mathcal{P}, \rho) - q^*U_{TP}(\mathcal{P}, \rho)$  in the considered case, such that both problem formulations lead the same optimal power allocation solution. As a result, we can focus on the equivalent objective function in the rest of the paper.

*B. Iterative Algorithm for Energy Efficiency Maximization*

In this section, an iterative algorithm (known as the Dinkelbach method [9]) is proposed for solving (9) with an equivalent objective function in subtractive form such that the obtained solution satisfies the conditions stated in Theorem 1. The proposed algorithm is summarized in Table I and the convergence to the optimal energy efficiency is guaranteed if the inner problem (12) can be solved in each iteration.

*Proof:* Please refer to [4, Appendix B] for a proof of convergence.

As shown in Table I, in each iteration in the main loop, i.e., lines 3–12, we solve the following optimization problem for a given parameter  $q$ :

$$\begin{aligned} & \max_{\mathcal{P}, \rho} U(\mathcal{P}, \rho) - qU_{TP}(\mathcal{P}, \rho) \\ & \text{s.t. C1, C2, C3, C4, C5, C6.} \end{aligned} \quad (12)$$

We note that  $U(\mathcal{P}, \rho) - qU_{TP}(\mathcal{P}, \rho) \geq 0$  holds for any value of  $q$  generated by Algorithm I. Please refer to [4, Proposition 3] for a proof.

*Solution of the Main Loop Problem:* The transformed problem has now an objective function in subtractive form which is less difficult to handle compared to the original formulation. However, there is still an obstacle in tackling the problem. The power splitting ratio  $\rho$  appears in the capacity equation in each subcarrier which couples the power allocation variables and results in a non-convex function, cf. (2). In order to derive a tractable power allocation algorithm, we have to overcome this problem. To this end, we perform a full search with respect to (w.r.t.)  $\rho$ . In particular, for a given value of  $\rho$ , we optimize the transmit power for energy efficiency maximization. We repeat the procedure for all possible values<sup>3</sup> of  $\rho$  and record the

<sup>3</sup>In practice, we discretize the range of  $\rho$ , i.e.,  $[0, 1]$ , into  $M \gg 1$  equally spaced intervals with an interval width of  $\frac{1}{M}$  for facilitating the full search.

in practical communication systems for the following reasons. First, it can be observed that  $\sum_{i=1}^{n_F} \epsilon P_i \geq \sum_{i=1}^{n_F} P_i > P_D$  due to path loss and the limited energy harvesting efficiency ( $\eta \leq 1$ ). Second, for achieving a reasonable system performance in communication, the interference level in the same channel has to be controlled (via regulation) to a reasonable level. Therefore, for a typical value of  $P_C$ ,  $P_C \gg P_I$  is always valid in practice.

The *energy efficiency* of the considered system is defined as the total average number of bits/Joule which is given by

$$U_{eff}(\mathcal{P}, \rho) = \frac{U(\mathcal{P}, \rho)}{U_{TP}(\mathcal{P}, \rho)}. \quad (8)$$

*B. Optimization Problem Formulation*

The optimal power allocation policy,  $\mathcal{P}^*, \rho^*$ , can be obtained by solving

$$\begin{aligned} & \max_{\mathcal{P}, \rho} U_{eff}(\mathcal{P}, \rho) \\ \text{s.t. C1: } & P_{\max}^{req} \geq P_D + P_I \geq P_{\min}^{req}, \\ \text{C2: } & \sum_{i=1}^{n_F} P_i \leq P_{\max}, \\ \text{C3: } & P_C + \sum_{i=1}^{n_F} \epsilon P_i \leq P_{PG}, \quad \text{C4: } \sum_{i=1}^{n_F} C_i \geq R_{\min}, \\ \text{C5: } & P_i \geq 0, \forall i, \quad \text{C6: } 0 \leq \rho \leq 1. \end{aligned} \quad (9)$$

Variable  $P_{\min}^{req}$  in C1 specifies the minimum required power transfer to the receiver.  $P_{\max}^{req}$  in C1 limits that maximum amount of harvested power because of the finite capacity of the battery. The value of  $P_{\max}$  in C2 puts a limit on the transmit spectrum mask to reduce the amount of out-of-cell interference. C3 is imposed to guarantee that the total power consumption of the system is less than the maximum power supply from the power grid  $P_{PG}$ , cf. Figure 1. C4 is the minimum required data rate  $R_{\min}$  whose values is provided by the application layer.

IV. SOLUTION OF THE OPTIMIZATION PROBLEM

The first step in solving the non-convex problem in (9) is to handle the objective function which comprises the ratio of two functions. We note that there is no standard approach for solving non-convex optimization problems in general. However, in order to derive an efficient power allocation algorithm for the considered problem, we transform the objective function using techniques from nonlinear fractional programming.

*A. Transformation of the Objective Function*

For the sake of notational simplicity, we first define  $\mathcal{F}$  as the set of feasible solutions of the optimization problem in (9) and  $\{\mathcal{P}, \rho\} \in \mathcal{F}$ . Without loss of generality, we denote  $q^*$  as the maximum energy efficiency of the considered system which is given by

$$q^* = \frac{U(\mathcal{P}^*, \rho^*)}{U_{TP}(\mathcal{P}^*, \rho^*)} = \max_{\mathcal{P}, \rho} \frac{U(\mathcal{P}, \rho)}{U_{TP}(\mathcal{P}, \rho)}. \quad (10)$$

We are now ready to introduce the following Theorem which is borrowed from nonlinear fractional programming [9].

*Theorem 1:* The maximum energy efficiency  $q^*$  is achieved if and only if

$$\begin{aligned} & \max_{\mathcal{P}, \rho} U(\mathcal{P}, \rho) - q^*U_{TP}(\mathcal{P}, \rho) \\ & = U(\mathcal{P}^*, \rho^*) - q^*U_{TP}(\mathcal{P}^*, \rho^*) = 0, \end{aligned} \quad (11)$$

for  $U(\mathcal{P}, \rho) \geq 0$  and  $U_{TP}(\mathcal{P}, \rho) > 0$ .

corresponding achieved energy efficiencies. At last, we select that  $\rho$  from all the trials which provides the maximum system energy efficiency. Note that for a fixed  $\rho$ , the transformed problem in (12) is concave w.r.t. the power allocation variables and (12) satisfies Slater's constraint qualification. As a result, the search space of the solution set can be reduced from  $n_F + 1$  dimensions (in problem (9)) to a one-dimensional search w.r.t.  $\rho$  due to the proposed transformation in Theorem 1 and dual decomposition which will be introduced in the next section.

Now, we solve the transformed problem for a given value of  $\rho$  by exploiting the concavity of the problem. It can be seen that strong duality holds for the transformed problem for a given value of  $\rho$ , then solving the dual problem is equivalent to solving the primal problem [10].

### C. Dual Problem Formulation

In this subsection, for a given value of  $\rho$ , we solve the power allocation optimization problem by solving its dual. For this purpose, we first need the Lagrangian function of the primal problem. The Lagrangian of (12) is given by

$$\begin{aligned} & \mathcal{L}(\alpha, \beta, \gamma, \lambda, \theta, \mathcal{P}, \rho) \\ &= \sum_{i=1}^{n_F} (1 + \gamma) C_i - q \left( U_{TP}(\mathcal{P}, \rho) \right) - \lambda \left( P_C + \sum_{i=1}^{n_F} \varepsilon P_i - P_{PG} \right) \\ & - \beta \left( \sum_{i=1}^{n_F} P_i - P_{\max} \right) - \gamma R_{\min} - \alpha \left( P_{\min}^{req} - P_D - P_I \right) \\ & + \theta \left( P_{\max}^{req} - P_D - P_I \right). \end{aligned} \quad (13)$$

Here,  $\lambda \geq 0$  is the Lagrange multiplier connected to C3 accounting for the power usage from the power grid.  $\beta \geq 0$  is the Lagrange multiplier corresponding to the maximum transmit power limit in C2.  $\alpha \geq 0$  and  $\gamma \geq 0$  are the Lagrange multipliers associated with the minimum required power transfer and the minimum data rate requirement in C1 and C4, respectively.  $\theta \geq 0$  is the Lagrange multiplier accounts for the maximum allowed power transfer in C1. On the other hand, boundary constraints C5 and C6 will be absorbed into the Karush-Kuhn-Tucker (KKT) conditions when deriving the optimal power allocation solution in the following.

The dual problem is given by

$$\min_{\alpha, \beta, \gamma, \lambda, \theta \geq 0} \max_{\mathcal{P}, \rho} \mathcal{L}(\alpha, \beta, \gamma, \lambda, \theta, \mathcal{P}, \rho). \quad (14)$$

### D. Dual Decomposition Solution

By Lagrange dual decomposition, the dual problem can be decomposed into two layers: Layer 1 consists of  $n_F$  subproblems with identical structure which can be solved in parallel; Layer 2 is the master problem. The dual problem can be solved iteratively, where in each iteration the transmitter solves the subproblems by using the KKT conditions for a fixed set of Lagrange multipliers, and the master problem is solved using the gradient method.

*Layer 1 (Subproblem Solution):* Using standard optimization techniques and KKT conditions, the optimal power allocation on subcarrier  $i$  for a given  $q$  is obtained as

$$P_i^* = \left[ \frac{W(1+\gamma)}{\ln(2)\Lambda_i} - \frac{1}{\Gamma_i} \right]^+, \quad \forall i, \quad \text{where} \quad (15)$$

$$\Lambda_i = q \left( \varepsilon - \eta \rho l g |H_i|^2 \right) + \lambda \varepsilon + \beta + (\theta - \alpha) \eta \rho l g |H_i|^2 \quad (16)$$

and  $[x]^+ = \max\{0, x\}$ . The power allocation solution in (15) is in the form of water-filling. Interestingly, the water-level in

(15), i.e.,  $\frac{W(1+\gamma)}{\ln(2)\Lambda_i}$ , is different across different subcarriers due to the *frequency selective power transfer efficiency* described after (6). On the other hand, Lagrange multipliers  $\gamma$  and  $\alpha$  force the transmitter to allocate more power for transmission to fulfill the data rate requirement  $R_{\min}$  and the minimum power transfer requirement  $P_{\min}^{req}$ , respectively.

*Layer 2 (Master Problem Solution):* The dual function is differentiable and, hence, the gradient method can be used to solve the Layer 2 master problem in (14) which leads to

$$\alpha(m+1) = \left[ \alpha(m) - \xi_1(m) \times \left( P_D + P_I - P_{\min}^{req} \right) \right]^+, \quad (17)$$

$$\beta(m+1) = \left[ \beta(m) - \xi_2(m) \times \left( P_{\max} - \sum_{i=1}^{n_F} P_i \right) \right]^+, \quad (18)$$

$$\gamma(m+1) = \left[ \gamma(m) - \xi_3(m) \times \left( \sum_{i=1}^{n_F} C_i - R_{\min} \right) \right]^+, \quad (19)$$

$$\lambda(m+1) = \left[ \lambda(m) - \xi_4(m) \times \left( P_{PG} - P_C - \sum_{i=1}^{n_F} \varepsilon P_i \right) \right]^+, \quad (20)$$

$$\theta(m+1) = \left[ \theta(m) - \xi_5(m) \times \left( P_{\max}^{req} - P_D - P_I \right) \right]^+, \quad (21)$$

where index  $m \geq 0$  is the iteration index and  $\xi_u(m)$ ,  $u \in \{1, 2, 3, 4, 5\}$ , are positive step sizes. Then, the updated Lagrange multipliers in (17)-(21) are used for solving the subproblems in (14) via updating the power allocation solution in (15).

Since the transformed problem is concave for given parameters  $q$  and  $\rho$ , it is guaranteed that the iteration between the Layer 2 master problem and the Layer 1 subproblems converges to the primal optimal solution of (12) in the main loop, if the chosen step sizes satisfy the infinite travel condition [10], [11].

After obtaining the solution of (12) with the above algorithm for a fixed  $\rho$ , we solve (12) again for another value of  $\rho$  until we obtain the energy efficiency for all considered values of  $\rho$ .

## V. RESULTS

In this section, we evaluate the performance of the proposed power allocation algorithm using simulations. The TGn path loss model [12] for indoor communication is adopted with 20 dB directional transmit and receive antennas gains. The distance between the transmitter and receiver is 10 meters. The system bandwidth is  $\mathcal{B} = 1$  MHz and the number of subcarriers is  $n_F = 128$ . We assume a carrier center frequency of 470 MHz which will be used by IEEE 802.11 for the next generation of Wi-Fi systems [13]. Each subcarrier for RF transmission has a bandwidth of  $W = 78$  kHz with antenna noise and signal processing noise powers of  $\sigma_{z_a}^2 = -128$  dBm and  $\sigma_{z_s}^2 = -125$  dBm [14], respectively. The small-scale fading coefficients of the transmitter and receiver links are generated as independent and identically distributed (i.i.d.) Rician random variables with Rician factor equal to 6 dB. Besides, the received interference at the receiver on each subcarrier is generated as i.i.d. Rayleigh random variables with variance specified in each case study. The shadowing of both the desired and interference communication links are set to 0 dB, i.e.,  $g = 1$  for the desired link. Unless specified otherwise, we assume a static signal processing power consumption of  $P_C = 40$  dBm, a minimum data rate requirement of  $R_{\min} = 10$  Megabits/s, a minimum required power transfer of  $P_{\min}^{req} = 0$  dBm, a maximum allowed power transfer of  $P_{\max}^{req} = 20$  dBm, and an energy harvesting efficiency of  $\eta = 0.8$ . We set  $M = 1000$  for discretizing the range of  $\rho$  into 1000 equally spaced intervals for performing the

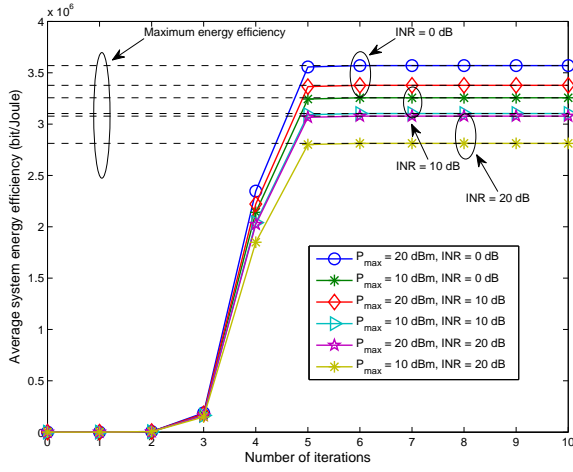


Fig. 2. Average system energy efficiency (bit/Joule) versus number of iterations for different levels of INR,  $\frac{\sigma_{I_i}^2}{\sigma_{z_s}^2}$ , and different values of maximum transmit power allowance,  $P_{\max}$ . The dashed lines represent the maximum energy efficiency for the different cases.

full search<sup>4</sup>. On the other hand, we assume a power efficiency of 38% for the power amplifier used at the transmitter, i.e.,  $\varepsilon = \frac{1}{0.38} = 2.6316$ . The average system energy efficiency is obtained by counting the number of bits which are successfully decoded by the receiver over the total power consumption averaged over multipath fading. Note that if the transmitter is unable to guarantee the minimum required data rate  $R_{\min}$  or the minimum required power transfer  $P_{\min}^{req}$ , we set the energy efficiency and the system capacity for that channel realization to zero to account for the corresponding failure. For the sake of illustration, we define the interference-to-signal processing noise ratio (INR) as  $\frac{\sigma_{I_i}^2}{\sigma_{z_s}^2}$ . In the following results, the “number of iterations” refers to the number of outer loop iterations of Algorithm 1 in Table I.

#### A. Convergence of Iterative Algorithm 1

Figure 2 illustrates the evolution of the average system energy efficiency of the proposed iterative algorithm for different levels of average received interference. In particular, we focus on the convergence speed of the proposed algorithm for a given value of optimal  $\rho$ . The results in Figure 2 were averaged over 100000 independent realizations for multipath fading. The dashed lines denote the average maximum energy efficiency for each case study. It can be observed that the iterative algorithm converges to the optimal value within 5 iterations for all considered scenarios. Besides, the variations in the INR level  $\frac{\sigma_{I_i}^2}{\sigma_{z_s}^2}$  and the maximum transmit power allowance  $P_{\max}$  have a negligible impact on the convergence speed of the proposed algorithm.

In the sequel, we set the number of iterations to 5 for illustrating the performance of the proposed algorithm.

#### B. Average Energy Efficiency

Figure 3 depicts the average system energy efficiency versus the maximum transmit power allowance,  $P_{\max}$ , for different received levels of interference. It can be seen that for  $P_{\max} < 10$  dBm, the system energy efficiency is zero since the optimization problem in (9) is infeasible due to an insufficient power transmission in the RF for satisfying the constraints on  $R_{\min}$  and  $P_{\min}^{req}$ . However, for a large enough  $P_{\max}$ , the energy efficiency of the proposed algorithm first increases with increasing  $P_{\max}$

<sup>4</sup>In practice, much smaller values for  $M$  (e.g.,  $M = 100$ ) can be used to reduce complexity at the expense of a small loss in performance.

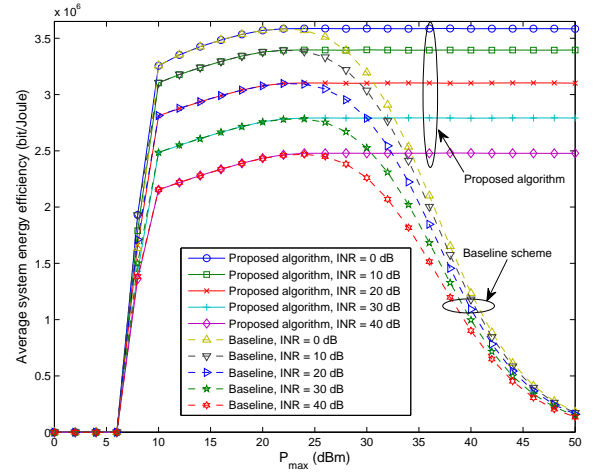


Fig. 3. Average system energy efficiency (bit-per-Joule) versus maximum transmit power allowance,  $P_{\max}$ , for different levels of INR,  $\frac{\sigma_{I_i}^2}{\sigma_{z_s}^2}$ .

and then approaches a constant as the energy efficiency gain due to a higher transmit power allowance gets saturated. This is because the transmitter is not willing to consume an exceedingly large amount of power for RF transmission, when the maximum system energy efficiency is achieved. Furthermore, the energy efficiency of the system is impaired by an increasing amount of interference, despite the potential energy efficiency gain due to energy harvesting from interference signals, cf. (6) and (8). For comparison, Figure 3 also contains the energy efficiency of a baseline power allocation scheme in which the system capacity (bit/s) with constraints C1–C6 in (9) is maximized. It can be observed that for the low-to-moderate maximum transmit power allowance regimes, i.e.,  $P_{\max} < 24$  dBm, the baseline scheme achieves the same performance as the proposed algorithm in terms of energy efficiency. This result indicates that in the low transmit power allowance regime, an algorithm which achieves the maximum system capacity may also achieve the maximum energy efficiency and vice versa. However, the energy efficiency of the baseline scheme decreases dramatically in the high transmit power allowance regime. This is because the baseline scheme employs a large transmit power for capacity maximization which is detrimental for energy efficiency maximization.

#### C. Average System Capacity

Figure 4 shows the average system capacity versus maximum transmit power allowance  $P_{\max}$  for different levels of INR,  $\frac{\sigma_{I_i}^2}{\sigma_{z_s}^2}$ . We compare the proposed algorithm again with the baseline scheme described in the last section. The average system capacities of both algorithms are zero for  $P_{\max} < 10$  dBm due to the infeasibility of the problem. For  $P_{\max} > 10$  dBm, it can be observed that the average system capacity of the proposed algorithm approaches a constant in the high transmit power allowance regime. This is because the proposed algorithm stops to consume more power for transmitting radio signals for maximizing the system energy efficiency. We note that, as expected, the baseline scheme achieves a higher average system capacity than the proposed algorithm in the high transmit power allowance regime. This is due to the fact that the baseline scheme consumes a larger amount of transmit power compared to the proposed algorithm. However, the baseline scheme achieves the maximum system capacity by sacrificing the system energy efficiency.

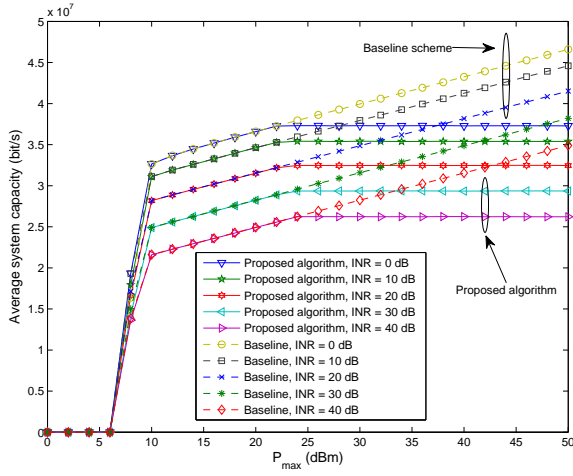


Fig. 4. Average system capacity (bit-per-second) versus maximum transmit power allowance,  $P_{\max}$ , for different levels of INR,  $\frac{\sigma_{I_i}^2}{\sigma_{z_s}^2}$ .

#### D. Average Harvested Power and Power Splitting Ratio

Figures 5 and 6 show, respectively, the average harvested power and the average optimal power splitting ratio,  $\rho$ , of the proposed algorithm versus maximum allowed transmit power,  $P_{\max}$ , for different levels of INR,  $\frac{\sigma_{I_i}^2}{\sigma_{z_s}^2}$ . It can be observed in Figure 5 that for small values of INR, i.e.,  $\text{INR} \leq 10$  dB, only a small amount of power is harvested by the receiver for energy efficiency maximization. In other words, a small portion of received power is assigned to the energy harvesting unit, cf. Figure 6. In fact, for small values of INR, assigning a larger amount of the received power for information decoding provides a higher capacity gain to the system which results in an improvement in energy efficiency. On the contrary, as shown in Figure 6, the receiver has a higher tendency to assigning a larger portion of the received power to the energy harvester in the interference limited regime, i.e.,  $\text{INR} \gg 10$  dB. Indeed, the SINR on each subcarrier approaches a constant in the interference limited regime and is independent of  $\rho$ , i.e.,  $\frac{(1-\rho)g|H_i|^2 P_i}{(1-\rho)(\sigma_{z_a}^2 + \sigma_{I_i}^2) + \sigma_{z_s}^2} \rightarrow \frac{P_i g |H_i|^2}{\sigma_{I_i}^2 + \sigma_{z_a}^2}$ . Thus, assigning more received power for information decoding does not provide a significant gain in channel capacity. On the contrary, the total power consumption decreases linearly w.r.t. an increasing  $\rho$ . As a result, assigning a larger portion of the received power to energy harvesting can enhance the system energy efficiency when the capacity gain is saturated in the interference limited regime.

## VI. CONCLUSIONS

In this paper, we formulated the power allocation algorithm design for simultaneous wireless information and power transfer in OFDM systems as a non-convex optimization problem. In the problem formulation, we took into account a minimum data rate requirement, a minimum required power transfer, and the circuit power dissipation. The multi-dimensional optimization problem was solved by using non-linear fractional programming, dual decomposition, and a one-dimensional full search. The simulation results reveal an interesting trade-off between energy efficiency, system capacity, and wireless power transfer.

## REFERENCES

- [1] T. Chen, Y. Yang, H. Zhang, H. Kim, and K. Horneman, "Network Energy Saving Technologies for Green Wireless Access Networks," *IEEE Wireless Commun.*, vol. 18, pp. 30–38, Oct. 2011.
- [2] O. Arnold, F. Richter, G. Fettweis, and O. Blume, "Power Consumption Modeling of Different Base Station Types in Heterogeneous Cellular Networks," in *Proc. Future Network and Mobile Summit*, 2010, pp. 1–8.

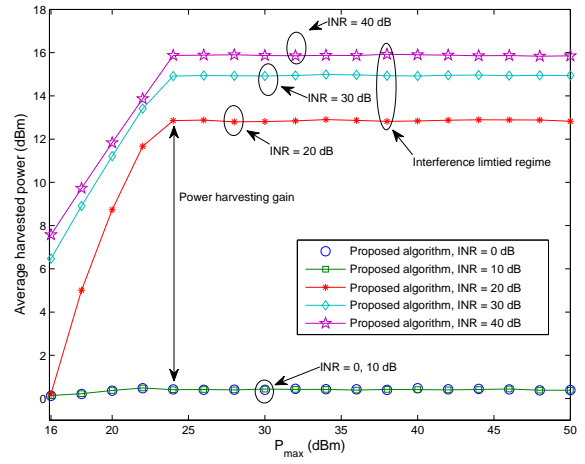


Fig. 5. Average harvested power (dBm) versus maximum transmit power allowance,  $P_{\max}$ , for different levels of INR,  $\frac{\sigma_{I_i}^2}{\sigma_{z_s}^2}$ . The double-sided arrow indicates the power harvesting gain due to an increasing  $\rho$  in the interference limited regime, cf. Figure 6.

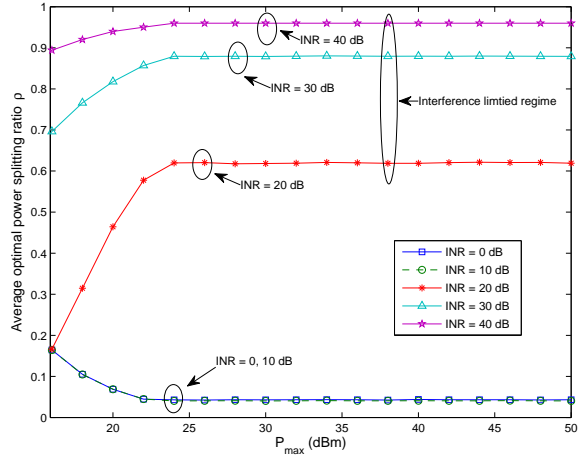


Fig. 6. Average optimal power splitting ratio,  $\rho$ , versus maximum transmit power allowance,  $P_{\max}$ , for different levels of INR,  $\frac{\sigma_{I_i}^2}{\sigma_{z_s}^2}$ .

- [3] J. Yang and S. Ulukus, "Optimal Packet Scheduling in an Energy Harvesting Communication System," *IEEE Trans. Commun.*, vol. 60, pp. 220–230, Jan. 2012.
- [4] D. W. K. Ng, E. Lo, and R. Schober, "Energy-Efficient Resource Allocation in OFDMA Systems with Large Numbers of Base Station Antennas," *IEEE Trans. Wireless Commun.*, vol. 11, pp. 3292–3304, Sept. 2012.
- [5] L. Varshney, "Transporting Information and Energy Simultaneously," in *Proc. IEEE Intern. Sympos. on Inf. Theory*, July 2008, pp. 1612–1616.
- [6] P. Grover and A. Sahai, "Shannon Meets Tesla: Wireless Information and Power Transfer," in *Proc. IEEE Intern. Sympos. on Inf. Theory*, 2010, pp. 2363–2367.
- [7] R. Zhang and C. K. Ho, "MIMO Broadcasting for Simultaneous Wireless Information and Power Transfer," in *Proc. IEEE Global Telecommun. Conf.*, Dec. 2011, pp. 1–5.
- [8] X. Zhou, R. Zhang, and C. K. Ho, "Wireless Information and Power Transfer: Architecture Design and Rate-Energy Tradeoff," Dec. 2012, accepted for presentation in the *IEEE Global Telecommun. Conf. 2012*, [Online] <http://arxiv.org/abs/1205.0618>.
- [9] W. Dinkelbach, "On Nonlinear Fractional Programming," *Management Science*, vol. 13, pp. 492–498, Mar. 1967. [Online]. Available: <http://www.jstor.org/stable/2627691>
- [10] S. Boyd and L. Vandenberghe, *Convex Optimization*. Cambridge University Press, 2004.
- [11] S. Boyd, L. Xiao, and A. Mutapcic, "Subgradient Methods," *Notes for EE392o Stanford University Autumn*, 2003–2004.
- [12] IEEE P802.11 Wireless LANs, "TGn Channel Models", IEEE 802.11-03/940r4, Tech. Rep., May 2004.
- [13] H.-S. Chen and W. Gao, "MAC and PHY Proposal for 802.11af," Tech. Rep., Feb., [Online] <https://mentor.ieee.org/802.11/dcn/10/11-10-0258-00-00af-mac-and-phy-proposal-for->
- [14] D. M. Pozar, *Microwave Engineering*, 3rd ed. New York: Wiley, 2005.